analytical chemistry

Article

Cite This: *Anal. Chem.* 2019, 91, 1203−1210

pubs.acs.org/ac

Imaging of Endogenous Hydrogen Peroxide during the Process of Cell Mitosis and Mouse Brain Development with a Near-Infrared Ratiometric Fluorescent Probe

Hailong Guo,[†] Guang Chen,*[,†,§] Min Gao,[†] Rui Wang,[†] Yuxia Liu,[†] and Fabiao Yu*[,†,‡]

[†]The Key Laboratory of Life-Organic Analysis, Key Laboratory of Pharmaceutical Intermediates and Analysis of Natural Medicine, College of Chemistry and Chemical Engineering, Qufu Normal University, Qufu 273165, China

[‡]Institute of Functional Materials and Molecular Imaging, College of Clinical Medicine, Key Laboratory of Hainan Trauma and Disaster Rescue, College of Emergency and Trauma, Hainan Medical University, Haikou 571199, China

[§]Laboratory of Tibetan Medicine Research & Qinghai Key Laboratory of Qinghai-Tibet Plateau Biological Resources, Northwest Institute of Plateau Biology, Chinese Academy of Science, Xining 810001, China

Supporting Information

ABSTRACT: Hydrogen peroxide (H_2O_2) is emerging as a new second messenger, which plays vital roles in intracellular signaling, thereby triggering physiological variations in terms of proliferation, differentiation, and migration. As known, cell mitosis has close association to the intracellular level of H_2O_2, which contribute to the significant effects on brain development, especially during the critical period of immaturity. Unfortunately, imaging H_2O_2 in a mammalian brain is still challenging. Herein, to further investigate the biological roles of endogenous H_2O_2 in cell mitosis, we develop a near-infrared ratiometric fluorescent probe Cy-PFS for specifically imaging endogenous H_2O_2 in cells and in vivo. Employing the probe Cy-PFS, we examine the critical effects of endogenous H_2O_2 on proliferation of cells in live hippocampal neurons cells, and our results provide strong evidence for H_2O_2 signaling in cell mitosis through growth factor signaling. Furthermore, we successfully demonstrate the close association of endogenous H_2O_2 level changes with the brain development at various stages. We envision that this present probe has potential as a promising useful chemical imaging tool for exploring the roles of H_2O_2 in cell mitosis.

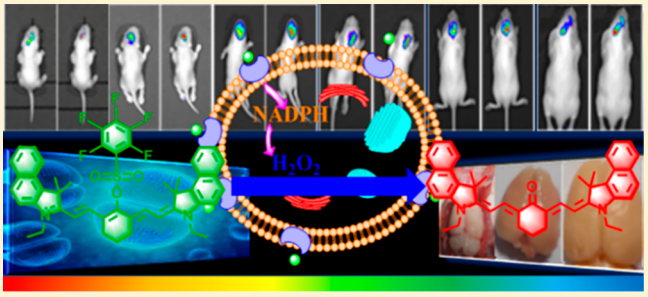

Endogenous hydrogen peroxide (H_2O_2) originates from the intracellular physiological stimulation. As a chemical second messenger in cells, H_2O_2 participates in a variety of biological processes in vivo, such as activation of immune cells,[1] remodeling of blood vessels,[2] and so on. The accumulating evidence imply that various growth factors and cytokines, including platelet-derived growth factor (PDGF), epidermal growth factor (EGF), insulin, and angiotensin II can promote the production of H_2O_2 in targeting cells under the regulation of nicotinamide adenine dinucleotide phosphate-oxidase (NADPH oxidase).[3] During the identification process between EGF and EGF receptor (EGFR), the endogenous H_2O_2 will trigger the self-phosphorylation of the particular tyrosine residues. The phosphorylation of certain signalling proteins usually leads to phosphorylation of downstream proteins, which contributes to the phosphorylation cascade reaction and activates the signaling pathway of PI3K,[4] thus involving the cell division. This signal transduction process is subjected to the inhibitive influence of phosphatase and tensin homologue (PTEN) deleted on chromosome. Such an inhibition blocks the forward signal of PI3K, thereby inhibiting the cell division.[5] However, the intracellular H_2O_2 can reversibly oxidize the PTEN into the disulfide and promotes the positive progress of the PI3K signaling pathway. Consequently, the transient increase of intracellular H_2O_2 may be necessary for mitosis.[6] Therefore, the detection of endogenous H_2O_2 with spatial−temporal accuracy is of significance for investigating the cell mitosis as well as the ontogenesis.

As a major member of reactive oxygen species (ROS), H_2O_2 transmits the membranes of living cells through free diffusion. It is difficult to detect intracellular H_2O_2 in situ. H_2O_2 easily reacts with biosubstances to form other ROS, and therefore, the methods for H_2O_2 detection require a fast response time. More importantly, there are many ROS that coexist in the living system, and high selectivity is also excepted to be achieved because H_2O_2 has lower reactivity than other highly ROS such as peroxynitrite ($ONOO^-$), hypochlorous acid (HOCl), hydroxyl radicals (·OH), and so on. Fluorescent bioimaging technology coupled with versatile chemo-probes

Received: November 17, 2018
Accepted: December 5, 2018
Published: December 5, 2018

DOI: 10.1021/acs.analchem.8b05326
Anal. Chem. 2019, 91, 1203−1210

Scheme 1. Molecular Structure of Probe Cy-PFS and the Proposed Mechanism toward H_2O_2

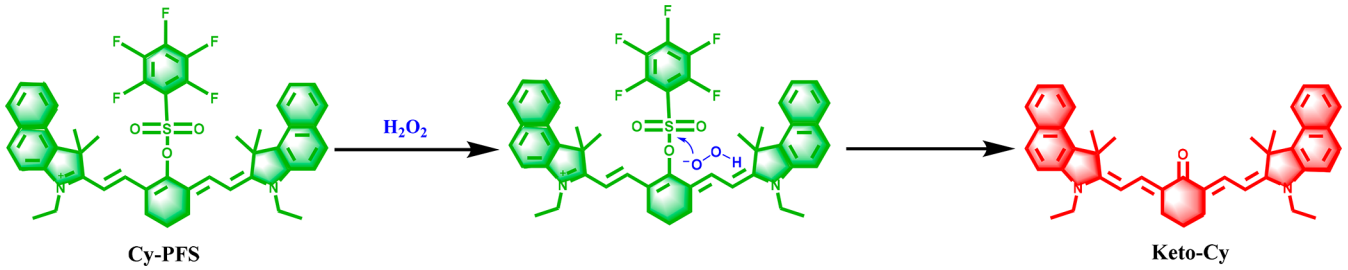

has been proved to be an efficient approach for examining the physiologically reactive species in living systems with high spatiotemporal resolution.[7−14] To confirm the H_2O_2-related physiological roles, a selective and sensitive fluorescent probe that meets the requirement of H_2O_2 analysis in real-time in living cells is highly desirable.[15] There are many molecular probes for endogenous H_2O_2 detection that have been elaborated,[10,16−20] but the detection mechanisms of these H_2O_2 probes are mainly based on boronate oxidation[8] or Baeyer−Villiger-type reactions.[9] To some extent, their reactivity, selectivity, and sensitivity must be improved for fulfilling the stringent issues of biological examination.[21,22] Therefore, the detection reactions that are suitable for the H_2O_2 probe design strategy are restricted in scope. Moreover, most of these probes allowed the insight of H_2O_2 in cells, and only a few probes have been applied for tissue imaging in vitro or in zebrafish.[19,20] As far as we know, no probe has been utilized for imaging of H_2O_2 in vivo, such as in mice. In comparison to the imaging of H_2O_2 in animals in real time, visualization of H_2O_2 in cells or tissues can only intuitively provide the intracellular H_2O_2 distribution in the local range and may not offer the long-term dynamic information during the physiological and pathological processes.[30] For imaging of H_2O_2 in vivo, a fluorescent probe with near-infrared (NIR) emission is necessary because the NIR fluorescence can penetrate deep tissue and prevent interference from self-background fluorescence.[23]

To accept the challenge, we herein designed a ratiometric near-infrared fluorescent probe (Cy-PFS) for imaging and evaluating endogenous H_2O_2 level changes during the cell mitosis and brain development processes. Cy-PFS could selectively and sensitively respond to H_2O_2 within 200 s without interferences of other ROS. The probe had good membrane permeability and could respond to the level changes of endogenous H_2O_2 in living cells. With the help of Cy-PFS, we confirmed the decisive effects of endogenous H_2O_2 on cell proliferation. The results revealed that the cells could produce H_2O_2 upon the stimulation of EGF, which achieved the strong evidence for H_2O_2 signaling in cell mitosis through growth factor signaling in live hippocampal neurons. Our probe exhibited deep tissue penetration for real-time imaging of H_2O_2 in mice models. We successfully detected the level changes of H_2O_2 in various development stages of mouse brain. The result of fluorescence images illustrated the close association of endogenous H_2O_2 with the brain development through promoting the cell mitosis for the first time.

EXPERIMENTAL SECTION

Synthesis of Cy-PFS. The synthesis procedures of other compounds were shown in Scheme S1. Keto-Cy (0.5 g, 0.7 mM) and pentafluobensulfonyl chloride (105 μL, 1.76 g/mL) was dissolved in 20 mL of anhydrous methylene chloride under Ar condition at 0 °C for 30 min. Then 50 μL of trimethylamine was added into the mixture. The reaction system was kept at 25 °C for 5 h. After the solvent was evaporated, the residues were purified by silica chromatography with ethyl acetate: methyl alcohol from 15:1 to 5:1 (v/v), and the green solid Cy-PFS was finally yielded (0.246 g, 35%).^{1}HNMR (500 MHz, $CDCl_3$-d_1) δ(ppm): 8.41 (d, J = 5.0, 2H), 8.12 (t, J = 25.0, 2H), 7.95−7.53 (m, 6H), 6.25 (dt, J = 5.0, 2H), 4.79 (dd, J_1 = 10.0, J_2 = 10.0, 4H), 2.80 (t, J = 10.0, 4H), 1.91 (s, 6H), 1.78 (s, 6H), 1.51 (t, J = 10.0, 6H), 1.36−1.33 (m, 2H). ^{13}CNMR (125 Hz, $CDCl_3$-d_1) δ(ppm): 177.49, 176.51, 167.72, 141.22, 140.41, 139.19, 137.43, 134.62, 133.03, 132.33, 132.05, 130.92, 130.16, 128.84, 127.66, 125.23, 122.08, 110.71, 101.03, 94.13, 65.56, 64.62, 51.10, 40.06, 31.87, 30.58, 29.67, 26.92, 19.19, 13.73, 12.53. LC-MS (ESI$^+$): m/z calcd for $C_{48}H_{44}F_5N_2O_3S^+$, 823.2987; found $[M]^+$, 822.8407.

HPLC Analyses. We used the HPLC technique to verify the response mechanism during the detection process between 10 μM probe with different concentration of H_2O_2 (from 0−100 μM), as shown in Figure S9.

Cell Imaging. Before our experiment, HL-7702 cell line (human normal liver cell line), A431 cell line (Epidermoid carcinoma cell line) and HT22 cell line (Hippocampal neuronal cell line) were cultured in 6-well Petri plates (∼ 2.0 × 10^5 cells/well) for 24 h at 37 °C and then treated as following steps. Cell images were obtained through confocal laserscanning microscope (Olympus FV1000) with an oil objective lens (60×). The fluorescence detection setting was kept constant through all imaging experiments.

Fluorescence Imaging of H_2O_2 Immature in BALB/c Mice Model. Since most of the brain development cycle in BALB/c mice started from birth to the fourth weeks,[24] we selected six groups of BALB/c mice, including 1-day, 3-day, 7-day, 14-day, 21-day, and 28-day. All the BALB/c mice were treated with intracranial injection of Cy-PFS (10 μM, 50 μL in 1:99 DMSO/saline, v/v).[25] Then the probe was intracranially incubated for 20 min, and the in vivo fluorescence images were acquired through PerkinElmer IVIS Lumina XR Series III system. Subsequently, changes in brain weights were obtained from each group. We used the percentage of brain weight relative to its weight as the analysis data to indicate the mouse brain development at different stages.[26] The important organs of mice were harvested to verify the images of our probe Cy-PFS in the brian. Each mouse was also treated with intracranial injection with the commercial ROS fluorescent probe 2,7-dichlorodihydrofluorescein (10 μM, 50 μL, in 1:99 DMSO/saline, v/v). Then the probe was intracranially incubated for 20 min. After these mice were euthanized, we took out the main organs and performed fluorescence imaging. All surgical procedures were conducted in conformity with National

DOI: 10.1021/acs.analchem.8b05326
Anal. Chem. 2019, 91, 1203−1210

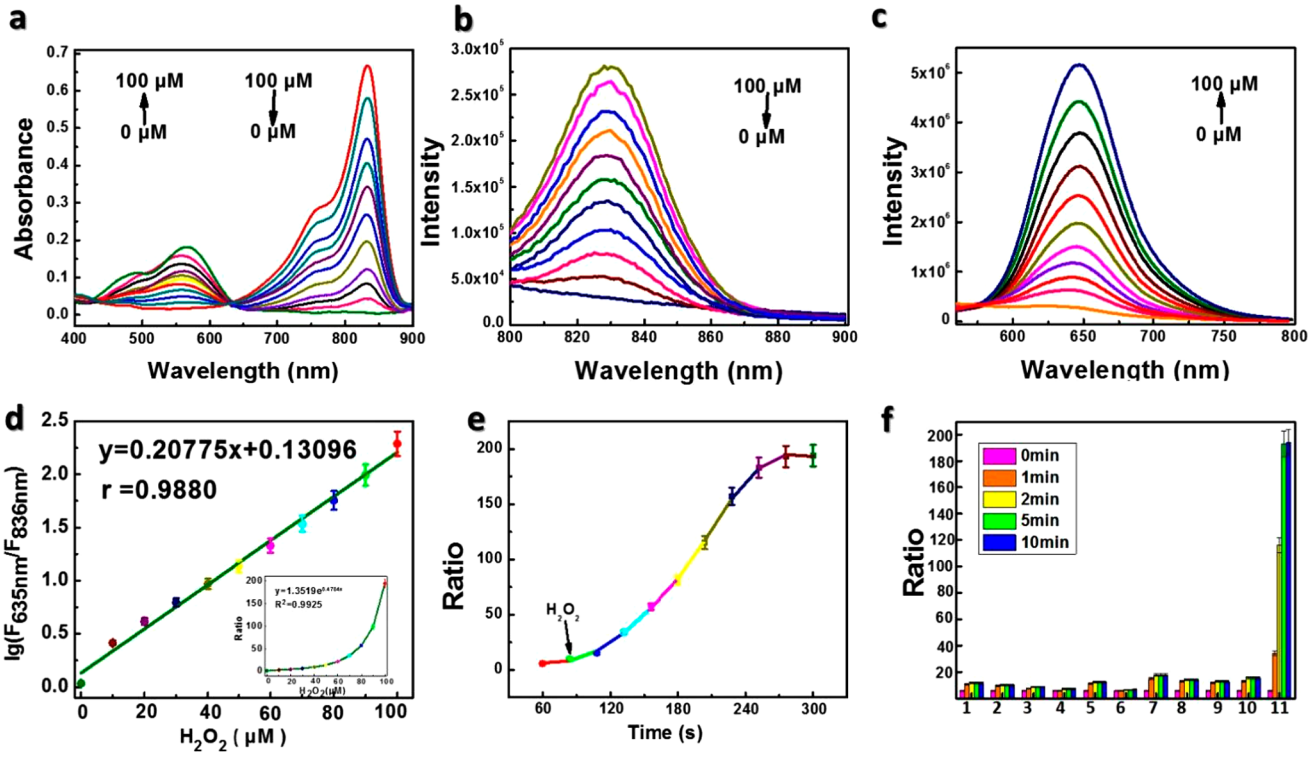

Figure 1. Spectral determination in 10 mM HEPES, pH 7.4, 37 °C. (a) UV absorption spectra of 10 μM Cy-PFS in presence with H_2O_2 (0−100 μM) for 10 min (b) and (c) were the fluorescence spectra changes of Cy-PFS toward H_2O_2 (0−100 μM). (d) The linear fitting curve between $\lg(F_{635}/F_{836})$ and H_2O_2 concentrations. Fluorescence intensity ratios were acquired after incubation with various concentrations of H_2O_2 for 10 min (e) Time-dependent intensity ratios of 10 μM Cy-PFS in the presence of 100 μM of H_2O_2. (f) Time-dependent fluorescent ratiometric response of 10 μM Cy-PFS toward various reactive oxygens/nitrogen and mercaptan species.1, 100 μM hypochlorite, 2, 100 μM hydroxyl radical, 3, 100 μM nitric oxide, 4, 100 μM superoxide anion, 5, 100 μM TBHP, 6, 100 μM singlet oxygen and 7, 100 μM tert-butyl hydroperoxide, 8, 100 μM glutamic acid, 9, 100 μM glutathione, 10, 100 μM cysteine, 11, 100 μM H_2O_2. The data were shown as mean (±SD) (n = 7).

Guidelines for the Care and Use of National Guidelines for the Care and Use of Laboratory Animals Laboratory Animals, and experimental protocols were approved by the Institutional Animal Care and Use Committee in Hainan Medical University, Haikou, China.

RESULTS AND DISCUSSION

Design and Synthesis of Probe Cy-PFS. The probe Cy-PFS was synthesized via the conjugation of a NIR benzohemicyanine platform with pentafluorobenzenesulfonyl chloride through a sulfonate linkage (Scheme 1). The NIR fluorophore cyanine-derivatives feature favorable optical properties involving NIR emission wavelength, relatively high absorption coefficient, outstanding biocompatibility, and low cytotoxicity. These characteristics make cyanine dyes an attractive candidate as chemical florescent probes for imaging of physiological reactive species in medicinal and biological investigation.[23,27,28] Moreover, the manipulation of the π-conjugation system of cyanine dyes will result in smart spectral emission regulation.[29−32] Spectral shifts often facilitates us to design ratiometric florescent probes, which will efficaciously eliminate data distortion caused by photobleaching, probe loading and retention, as well as device factors, such as lighting stability.[29−32] As reported, H_2O_2 undergoes a highly selective perhydrolysis reaction of acyl derivatives.[10] The designed pentafluorobenzenesulfonyl group is more stable to hydrolysis than ester bond, and the pentafluorobenzene ring enhances the reactivity of the sulfonates toward H_2O_2.[33] As shown in Scheme 1, our probe Cy-PFS possessed a NIR wavelength and was suitable for the in vivo imaging analysis. After selectively deprotecting the pentafluorobenzenesulfonyl group by H_2O_2, the π-conjugation system was rearranged, thus promising to release the emission at different wavelengths.

Spectroscopic Properties and Selectivity of Cy-PFS. With the probe Cy-PFS in hand, we then tested its spectroscopic properties. The fluorescence and absorption spectra were measured under simulated physiological conditions (Cy-PFS 10 μM, 10 mM HEPES, pH 7.4, 37 °C). As displayed in Figure 1a, the probe Cy-PFS itself showed the maximal absorbance centered at 830 nm. Upon the addition of H_2O_2, a new absorbance centered at 560 nm emerged. With the excitation at 730 nm, the probe Cy-PFS offered fluorescence emission centered at 836 nm. With the increasing amount of additional H_2O_2, the emission profile decreased (Figure 1b). Correspondingly, the fluorescence emission centered at 635 nm was increased with the excitation of 560 nm. Therefore, a NIR ratiometric pattern could be established with the employment of different changes in spectra emission (Figure 1c). The logarithm of fluorescence ratio (I_{635}/I_{836}) displayed a good linear relationship with the addition of 0−100 μM H_2O_2 (Figure 1d). The regression equation was Lg(Ratio) = 0.20775 [H_2O_2] + 0.13096, with r = 0.9880. The limit of detection for H_2O_2 detection was calculated to be as 50 nM. Then we measured the ratio signal vs the reaction time between 10 μM probe and 100 μM H_2O_2. It indicated that the probe offered a fast reaction kinetics within 200 s (Figure 1e). The pseudo-first order rate constant was determined to be k = 6.9 × 10^{-3} s^{-1}. Since there were many reactive oxygens/

DOI: 10.1021/acs.analchem.8b05326
Anal. Chem. 2019, 91, 1203−1210

nitrogen and mercaptan species in cells, the specific detection ability to H_2O_2 was crucial for our probe. To test the selectivity of Cy-PFS, we investigated various reactive oxygens/nitrogen species (hypochlorite, hydroxyl radical, singlet oxygen, superoxide anion, tert-butyl hydroperoxide, nitric oxide, and peroxynitrite at 100 μM) and mercaptan (glutathione, cysteine, and glutamic acid at 100 μM). As shown in Figure 1e, the ratiometric signals showed negligible changes for these reactive species. Whereas, there was a large ratiometric response in the presence of H_2O_2. Therefore, the probe Cy-PFS could be employed for the selective detection of H_2O_2.

Imaging of H_2O_2 in HL-7702 Cells. We chose the normal human liver HL-7702 cell line as a representative cell model to test the applicability of Cy-PFS in cells.[1,34] As shown in Figure 2, the HL-7702 cells in group a - d were incubated with 1 μM

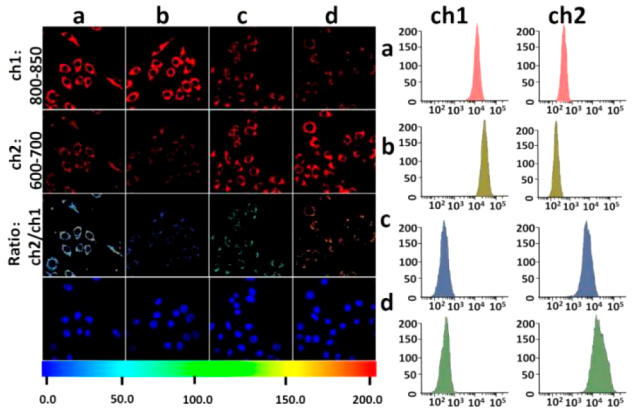

Figure 2. Detection of exogenous H_2O_2 in HL-7702 cells through confocal microscopy and flow ctyometric. HL-7702 cells were incubated with 1 μM of Cy-PFS for 15 min at 37 °C before imaging. Fluorescence collection windows ch 1: λ_{ex} = 750 nm, λ_{em} = 800−850 nm; ch 2: λ_{ex} = 545 nm, λ_{em} = 600−700 nm; Nucleus dye Hoechst 33258: λ_{ex} = 405 nm, λ_{em} = 410−510 nm. (a) Control. (b) HL-7702 cells were incubated with 100 μM of PD153035 at 37 °C for 25 min (c) Cells were treated as described in b, and then 30 μM H_2O_2 was added. (d) Cells were treated as described in (b), then added 50 μM H_2O_2. Scale bar = 10 μm. The data were shown as mean (± SD) (n = 7).

of Cy-PFS at 37 °C for 15 min before fluorescence imaging. The fluorescence images were collected from two fluorescence collection windows, channel 1 (ch1): λ_{ex} = 750 nm, λ_{em} = 800−850 nm; channel 2 (ch 2): λ_{ex} = 545 nm, λ_{em} = 600−700 nm. Pseudocolor ratio images were reconstructed to represent the ratio emission intensity in channel 2 images and in channel 1 images at the same time point. Group a was the control. The HL-7702 cells in group b were treated with 100 μM PD153035 (an EGFR kinase domain)[35] at 37 °C for 25 min to increase the level of intracellular H_2O_2. The group c HL-7702 cells were pretreated as describe in group b, and then 30 μM of H_2O_2 was added. The HL-7702 cells in group d were performed as described in group c, and then 50 μM of H_2O_2 was added. As shown in Figure 2a, ch 1 showed strong fluorescence, whereas ch 2 showed weak florescence, and the faint ratio image implied the low level of intracellular endogenous H_2O_2. After the cells were pretreated with PD153035 (100 μM) for 25 min, the cells in Figure 2b provided a rather lower ratio image than group a. This result indicated that the endogenous level of H_2O_2 was remarkably inhibited by PD153035. To further confirm the above result, we added 30 μM H_2O_2 into the cell dish of group c (Figure 2c). As expected, the ch 1 emitted the weaker fluorescence emission, and ch 2 gave the obviously stronger emission than those in Figure. 2b. Simultaneously, we obtained a bright ratio image of the cells in group c. The cells in group d were incubated with exogenous 50 μM H_2O_2. As displayed in Figure 2d, the ch 1 emitted weak fluorescence, and ch 2 demonstrated a quite strong fluorescence. The above experiments demonstrated that the probe Cy-PFS was able to detect the exogenous H_2O_2 in cells. Besides, we performed the flow cytometry analysis to confirm the above results. The fluorescence intensity changes in ch 1 and ch 2 showed the satisfactory consistency to the results from cell imaging. The costaining of Cy-PFS in ch 1 and Hoechst 33258 (a nucleus dye) revealed that our probe localized in the cytoplasm.

Effects of Endogenous H_2O_2 for Cell Proliferation. The experiments with HL-7702 cells demonstrated the potential applicability of our probe Cy-PFS for exploring the roles of the intracellular H_2O_2. We next wanted to detect the endogenous level changes of H_2O_2 during cell proliferation. We selected human epidermoid carcinoma A431 cell line as the testing model. In the surface membrane of A431 cells, there exists a large number of EGFR for accepting EGF.[36] The combination between EGF and EGFR can activate NADPH, thereby releasing H_2O_2.[37] The resulting H_2O_2 will induce rapid tyrosine phosphorylation of intracellular signaling proteins which contribute to cellular proliferation processes.[38] The A431 cells in Figure 3 were divided into six groups. All the A431 cells were incubated with 1 μM Cy-PFS at 37 °C for 15 min before imaging. Fluorescence images were collected via a laser-scanning microscope. The fluorescence collection windows were set as follows. For the probe Cy-PFS, channel 1 (ch1): λ_{ex} = 750 nm, λ_{em} = 800−850 nm; channel 2 (ch 2): λ_{ex} = 545 nm, λ_{em} = 600−700 nm. For a commercial ROS probe 2, 7-dichlorodihydrofluorescein, ch 3: λ_{ex} = 488 nm, λ_{em} = 500−530 nm. Group a was as control. The A431 cells in group b were treated with 500 ng/mL EGF for 15 min at 37 °C. Group c was pretreated with 100 μM PD153035 at 37 °C for 25 min and then incubated with 500 ng/mL EGF for 15 min. Group d was pretreated with 100 μM wortmannin[39] at 37 °C for 25 min and then treated with 500 ng/mL EGF for 15 min. The next A431 cells in group e were pretreated with 100 μM of apocynin[40] at 37 °C for 25 min and then incubated with 500 ng/mL EGF for 15 min. Group e was pretreated with 100 μM NG-Nitro-L-arginine methyl ester hydrochloride (L-NAME)[41] at 37 °C for 25 min and then treated with 500 ng/mL EGF for 15 min. As shown in Figure 3a, the fluorescence ratio images indicated the endogenous level of H_2O_2 in the A431 cells. Additionally, the treatment EGF (500 ng/mL) would obviously induce the production of H_2O_2 (Figure 3b). The result demonstrated that EGF could up-regulate the level of endogenous H_2O_2. To confirm this result, we next performed an EGFR inhibition experiment. After pretreating the cells in group c with the EGFR specific inhibitor PD153035 (100 μM), even the stimulation with EGF (500 ng/mL) could not increase the level of intracellular H_2O_2 (Figure 3c). The result indicated that PD153035 could inhibit the combination between EGF and EGFR. PI3K (phosphatidylinositide 3-kinases) is the enzyme involved in cellular functions such as cell growth, proliferation, differentiation, and motility.[42] We performed another inhibition experiment to verify the roles of P13K in the EGF-EGFR-P13K procedure. A P13K inhibitor Wortmannin (100 μM) was used to inhibit the self-phosphorylation process. The low ratio fluorescence images

DOI: 10.1021/acs.analchem.8b05326
Anal. Chem. 2019, 91, 1203−1210

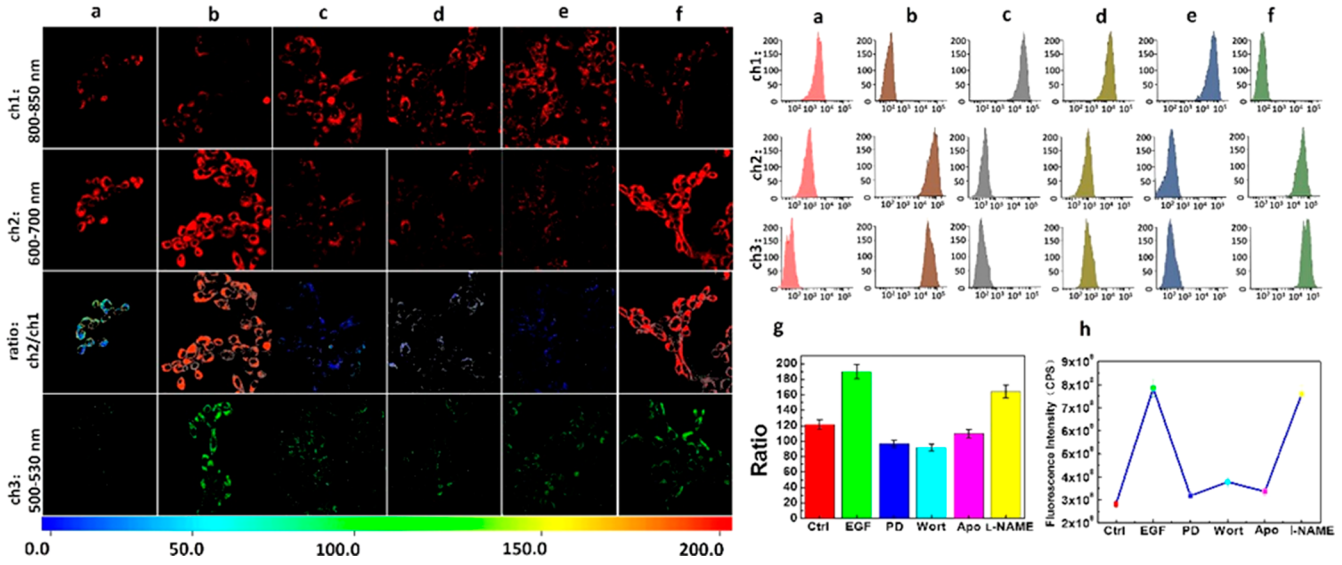

Figure 3. Detection of endogenous H2O2 in A431 cells through confocal microscopy and flow ctyometric. Fluorescence collection windows: ch 1: λ_{ex} = 750 nm, λ_{em} = 800−850 nm; ch 2: λ_{ex} = 545 nm, λ_{em} = 600−700 nm. ch 3: λ_{ex} = 488 nm, λ_{em} = 500−530 nm. Nucleus dye Hoechst 33258: λ_{ex} = 405 nm, λ_{em} = 410−510 nm. (a) A431 cells were incubated with 1 μM of Cy-PFS for 15 min at 37 °C. (b) A431 cells were incubated with EGF (1 μg/mL) for 15 min. (c) Cy-PFS-labeled A431 cells were pretreated with PD153035 before EGF (1 μg/mL) stimulation. (d) Cy-PFS-labeled A431 cells were pretreated with wortmannin before EGF stimulation. (e) Cy-PFS-labeled A431 cells pretreated with apocynin incubated before EGF stimulation. (f) Cy-PFS-labeled A431 cells were pretreated with L-NAME before EGF stimulation. As shown in the figure, we also performed the flow cytometric analysis of a−f cells. (g) The fluorescence ratio values of Cy-PFS in a−f. (h) The fluorescence intensity of commercial probe 2,7-dichlorodihydrofluorescein in a−f. Scale bar = 20 μm. The data were shown as mean (± SD) (n = 7).

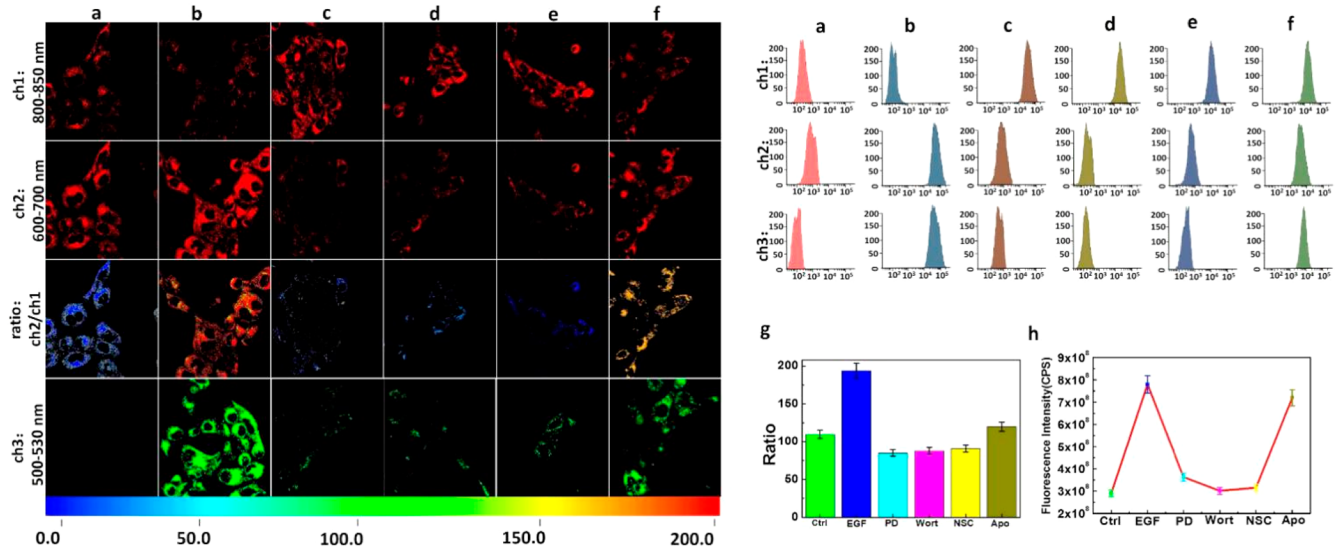

Figure 4. Detection of endogenous H2O2 in HT22 cells through confocal microscopy and flow ctyometric. Fluorescence collection windows: ch 1: λ_{ex} = 750 nm, λ_{em} = 800−850 nm; ch 2: λ_{ex} = 545 nm, λ_{em} = 600−700 nm. ch 3: λ_{ex} = 488 nm, λ_{em} = 500−530 nm. Nucleus dye Hoechst 33258: λ_{ex} = 405 nm, λ_{em} = 410−510 nm. (a) HT22 cells were incubated with 1 μM of Cy-PFS for 15 min. (b) Cy-PFS-labeled HT22 cells were incubated with EGF (1 μg/mL) for 15 min. (c) Cy-PFS-labeled HT22 cells were pretreated with PD153035 before EGF (1 μg/mL) stimulation. (d) Cy-PFS-labeled HT22 cells pretreated with wortmannin before EGF (1 μg/mL) stimulation. (e) Cy-PFS-labeled HT22 cells pretreated with NSC23766 before EGF (1 μg/mL) stimulation. (f) Cy-PFS-labeled HT22 cells pretreated with apocynin before EGF stimulation. The flow cytometric analysis of a−f cells were performed as shown in the figure. (g) The fluorescence ratio values of Cy-PFS in a−f. (h) The fluorescence intensity of commercial probe 2, 7-dichlorodihydrofluorescein in a−f. Scale bar = 20 μm. The data were shown as mean (± SD) (n = 7).

in Figure 3d illustrated the decreasing level of endogenous H_2O_2 as the result of PI3K inhibition. Alternatively, the endogenous H_2O_2 could be generated via the activation of the NADPH oxidase, which derived us to carry out the investigation for NADPH-dependent H_2O_2 production. Apocynin was used to inhibit the activity of NADPH oxidase. The faint ratio images in Figure 3e demonstrated the decrease of the NADPH-dependent H_2O_2 level in the tested cells. To exclude the potential interferences from other reactive nitrogen species in cells, we then performed the additional inhibition examination of nitric oxide synthase. The cells in group f was treated with L-NAME (100 μM) to inhibit the activity of nitric oxide synthase. The results in Figure. 3f indicated that the detection of endogenous H_2O_2 was not interfered by the

DOI: 10.1021/acs.analchem.8b05326
Anal. Chem. 2019, 91, 1203−1210

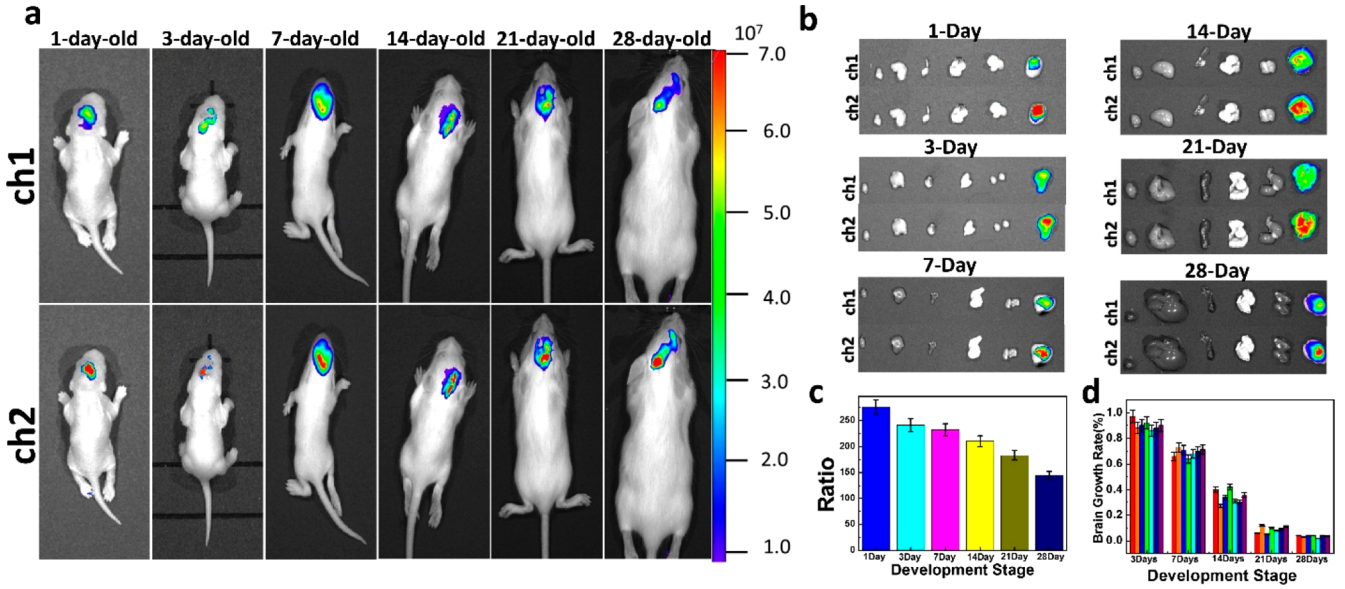

Figure 5. (a) Fluorescence imaging of H2O2 in the hippocampus of various development mouse. (ch 1: λ_{ex} = 730 nm, λ_{em} = 760−840 nm; ch 2: λ_{ex} = 540 nm, λ_{em} = 620−670 nm. BALB/c mice of 1-day-old, 3-day-old, 7-day-old, 14-day-old, 21-day-old, and 28-day-old. (b) The fluorescence detection of vitro vital organs from the mouse in panel a. From left to right, in turn, heart, liver, spleen, lung, kindey, and brain. (c) The fluorescence ratio signals of H_2O_2 detection in mouse hippocampus at different developmental stages. The mouse developmental status by measuring the percentage of mouse brain weight. All the above experiments were incubated with Cy-PFS (10 μM, 50 μL in 1:99 DMSO/saline, v/v). The data were shown as mean (± SD) (n = 7).

intracellular reactive nitrogen species. We also utilized a commercial probe 2,7-dichlorodihydrofluorescein to detect the level changes of H_2O_2. As shown in Figure 3, the results from ch 3 revealed that the commercial ROS fluorescent probe 2,7-dichlorodihydrofluorescein hardly detect the intracellular endogenous H_2O_2 concentration, it only could be used to detect a high level of H_2O_2 in cells. While our probe could be used to reveal the level changes of endogenous H_2O_2. The result confirmed that our probe had high sensitivity for the detection of endogenous H_2O_2 in cells under the same testing conditions. The trend of H_2O_2 level changes were also presented in histogram for a direct comparison (Figure 3g,h) Fluorescence images of the nucleus by Hoechst 33258 and the bright field were shown in Figure S4.

Imaging of H_2O_2 Generation upon EGF Stimulation. Our final aim was to perform in vivo imaging analysis of H_2O_2 generation in the brain. Before the in vivo application, we selected a mouse hippocampal neuron HT22 cell line as the representative cell model to examine the level changes of H_2O_2 under the EGF stimulation.[43] We performed six parallel experiments using HT22 cells (Figure 4). All the HT22 cells were incubated with 1 μM Cy-PFS at 37 °C for 15 min before imaging. Group a was as control. Group b was pretreated with 500 ng/mL EGF for 15 min at 37 °C and then imaging. The HT22 cells in group c were pretreated with 100 μM of PD153035 at 37 °C for 25 min and then with 500 ng/mL EGF for 15 min. Group d was pretreated with 100 μM of wortmannin at 37 °C for 25 min and then with 500 ng/mL EGF for 15 min. Group e was pretreated with first 100 μM of NSC23766 (a selective inhibitor of Rac1)[44] at 37 °C for 25 min and then 500 ng/mL EGF for another 15 min. The last group was pretreated with 100 μM of apocynin (a selective inhibitor of NADPH oxidase) at 37 °C for 25 min and then with the 500 ng/mL EGF for 15 min. The ratio fluorescence image of group a implied the endogenous H_2O_2 in HT22 cells. The cells in Figure 4b emitted a strong ratio fluorescence image, indicating that the H_2O_2 was elevated with the inductive effect of between EGF and EGFR. As a controlled trial, the cells in Figure 4c offered a remarkably lower ratio image than in Figure 4b, and the result illustrated that the inhibition of EGFR with PD153035 (100 μM) would decrease the generation of H_2O_2 when stimulated with EGF. To further verify the above results, we next performed the PI3K inhibition experiment utilizing wortmannin (Figure 4d). The result indicated that the endogenous H_2O_2 was down-regulated by the inhibitive effect of wortmannin. We next performed a Rac1-NADPH signal pathway inhibition experiment. After they were incubated with the inhibitor NSC23766 (100 μM) for Rac1, the cells in Figure 4e showed the weak ratio fluorescence image. Clearly, the NSC23766 inhibited the Rac1-NADPH signal pathway thereby down-regulated the endogenous H_2O_2. We also performed an experiment with NADPH inhibitor to hinder the Rac1-NADPH signal. As shown in Figure 4f, with the addition of 100 μM of apocynin, the cells provided the obviously weak ratio fluorescence intensity. Therefore, the endogenous H_2O_2 generated form the Rac1-NADPH signal pathway was reduced. Moreover, to further validate the capability of our probe for the detecting intracellular H_2O_2 level, we used a commercial ROS fluorescent probe 2,7-dichlorodihydrofluorescein as a control probe for imaging of the intracellular H_2O_2. As shown in Figure. 4, the results from ch 3 demonstrated that the commercial ROS fluorescent probe 2,7-dichlorodihydrofluorescein hardly detected the intracellular background H_2O_2 concentration, it only could be used to detect high level of H_2O_2 in cells. While our probe could be used to reveal the level changes of endogenous H_2O_2. The result confirmed that our probe had high sensitivity for the detection of endogenous H_2O_2 in cells under the same testing conditions. We performed the flow cytometry analysis for verifying the results obtaining from confocal microscopy. The average ratios of fluorescence intensities (I_{ch2}/I_{ch1}) were displayed in Figure 4g,h for directly quantify the concentration

DOI: 10.1021/acs.analchem.8b05326
Anal. Chem. 2019, 91, 1203−1210

of endogenous H_2O_2. Fluorescence imaging of the nucleus by Hoechst 33258 and the bright field were shown in Figure S5.

Evaluation of H_2O_2 Level during Brain Development Process. Since the above experiments demonstrated that the probe Cy-PFS could be used to detect H_2O_2 in cells, we next wanted to detect H_2O_2 in vivo. Cell mitosis plays crucial roles in brain development of the neonatal mammals. The brain development of the neonatal mammals as well as the cell mitosis are in rapid growth after birth,[24] which may be closely associated with the high lelve of endogenous H_2O_2.[45,46] For the brain of newborn BALB/c mice models, the rapid brain development was mainly in the first 4 weeks after birth, especially in the first 2 weeks after birth. The newly born mice were divided into six groups according to the birth time, including 1-day-old, 3-day-old, 7-day-old, 14-day-old, 21-day-old, and 28-day-old. All the BALB/c mice were treated with intracranial injection of the probe Cy-PFS (10 μM, 50 μL, in 1:99 DMSO/saline, v/v). Twenty minutes later, the mice in Figure 5 were exposed to small living animal imaging system for the further in vivo imaging analysis. Our results revealed that there were obvious differences in the level of endogenous H_2O_2 during the different developmental stages of the brain. As shown in Figure 5a, in the brain of the1-day-old mice, ch 2 had very strong fluorescence intensity, implying the high level of endogenous H_2O_2. As expected, in the 3-day-old mice, ch 2 provided a relatively weaker fluorescence intensity, which indicated that the level of endogenous H_2O_2 was down-regulated. Although there was still a relatively high level of endogenous H_2O_2 in the brain of 14-day-old mice, the developmental speed was slowed down compared with those of 1-day-old mice and 3-day-old mice. Furthermore, the decreasing trends of endogenous H_2O_2 in the brain were continuous in the groups of 21-day-old mice and 28-day-old mice. To further confirm our results, we harvested the different organs and performed imaging analysis (Figure 5b). Under the same test parameters of the instrument, the heart, liver, spleen, lung, and kidney could not be detected fluorescence intensity, except for the brain. We also employed the commercial probe (2,7-dichlorodihydrofluorescein, 10 μM, 50 μL, in 1:99 DMSO/saline, v/v) for the evaluation of the level of endogenous H_2O_2 in mice brain under the same conditions. Because the short fluorescence emission of the commercial probe limited its direct fluorescence imaging in vivo, we carried out the isolated organ imaging in vitro. As shown in Figure S6, Figure S7, the fluorescence was collected, but the observed fluorescence intensity was obviously low. Depending on the collected signals from the two channels in Figure 5a. The ratiometric data were provided in Figure 5c. As expected, the fluorescence ratios displayed good consistency with those of the commercial probe. With the in vivo and in vitro imaging analysis, we hypothesized that the descending endogenous H_2O_2 implied the slowing down trend of brain development. Since the endogenous H_2O_2 has been suggested to promote cell mitosis and may positively control brain development. The percentage of naked brain mass to body weight was selected as the development index.[24] Additionally, the brain growth rate of the 1-day-old mouse was set as 1. As shown in Figure 5d, obviously, during the first 4 weeks, the mouse brain was undergoing vigorous division and development, and the developmental speed was higher in the first 2 weeks than that in the last 2 weeks. These results were in good agreement with the level of endogenous H_2O_2, which confirmed the in vivo imaging from the physiological aspect. All the experimental results demonstrated that the probe Cy-PFS could be used for exploring the endogenous H_2O_2 in cells and in vivo.

CONCLUSIONS

In summary, we designed and synthesized a ratiometric near-infrared probe Cy-PFS for the detection of endogenous H_2O_2 generated from cell signaling in cells and in vivo. The versatile regulation of the enlarged π-conjugation system in Cy-PFS by the pentafluorobenzenesulfonyl group results in a selective H_2O_2 ratiometric probe with two different near-infrared fluorescence emission. The probe Cy-PFS provides strong evidence for H_2O_2 signaling in cell mitosis. Moreover, we successfully detected the level changes of H_2O_2 at various stages of brain development in mice. The results for the first time illustrated the close relationship between endogenous H_2O_2 and brain development through promoting cell mitosis. This work may provide further information for exploring H_2O_2 as a chemical messenger molecule in cell mitosis.

ASSOCIATED CONTENT

Supporting Information

The Supporting Information is available free of charge on the ACS Publications website at DOI: 10.1021/acs.analchem.8b05326.

More experimental materials and details, synthesis steps, and characterization of compounds (PDF)

AUTHOR INFORMATION

Corresponding Authors

*E-mail: fbyu@yic.ac.cn. Tel./Fax: (+86)-0898-66892503.
*E-mail: chenandguang@163.com

ORCID

Guang Chen: 0000-0002-0454-1686
Fabiao Yu: 0000-0003-0073-6299

Notes

The authors declare no competing financial interest.

ACKNOWLEDGMENTS

We thank the National Nature Science Foundation of China (Nos. 21775162 and 21864011), China Postdoctoral Science Foundation (Grant 2017M622254), Natural Science Foundation of Shandong Province (Grant ZR201709240033), Talent Program of Hainan Medical University (Grants XRC180006 and XRC180007), and Hundred-Talent Program (Hainan 2018).

REFERENCES

(1) Reth, M. *Nat. Immunol.* **2002**, *3*, 1129−1134.
(2) Conklin, D. J.; Cowley, H. R.; Wiechmann, R. J.; Johnson, G. H.; Trent, M. B.; Boor, P. J. *Am. J. Physiol-heart C* **2004**, *286*, H667−H676.
(3) Rhee, S. G. *Science* **2006**, *312*, 1882−1883.
(4) Rhee, S. G.; Bae, Y. S.; Lee, S. R.; Kwon. *Sci. Signaling* **2000**, *2000*, pe1.
(5) Carracedo, A.; Pandolfi, P. P. *Oncogene* **2008**, *27*, 5527−5541.
(6) Rhee, S. G.; Chang, T. S.; Bae, Y. S.; Lee, S. R.; Kang, S. W. *J. Am. Soc. Nephrol.* **2003**, *14*, S211−S215.
(7) Zhao, X.; Li, M.; Sun, W.; Fan, J.; Du, J.; Peng, X. *Chem. Commun.* **2018**, *54*, 7038−7041.
(8) Ren, T. B.; Xu, W.; Zhang, W.; Zhang, X. X.; Wang, Z. Y.; Xiang, Z.; Yuan, L.; Zhang, X. *J. Am. Chem. Soc.* **2018**, *140*, 7716−7722.

DOI: 10.1021/acs.analchem.8b05326
Anal. Chem. 2019, 91, 1203−1210

(9) Jiao, X.; Xiao, Y.; Li, Y.; Liang, M.; Xie, X.; Wang, X.; Tang, B. *Anal. Chem.* **2018**, *90*, 7510−7516.
(10) Dong, B.; Song, X.; Kong, X.; Wang, C.; Tang, Y.; Liu, Y.; Lin, W. *Adv. Mater.* **2016**, *28*, 8755−8759.
(11) Yin, J.; Kwon, Y.; Kim, D.; Lee, D.; Kim, G.; Hu, Y.; Ryu, J.-H.; Yoon, J. *J. Am. Chem. Soc.* **2014**, *136*, 5351−5358.
(12) Gu, K.; Xu, Y.; Li, H.; Guo, Z.; Zhu, S.; Zhu, S.; Shi, P.; James, T. D.; Tian, H.; Zhu, W. H. *J. Am. Chem. Soc.* **2016**, *138*, 5334−5340.
(13) Chen, X.; Lee, D.; Yu, S.; Kim, G.; Lee, S.; Cho, Y.; Jeong, H.; Nam, K. T.; Yoon, J. *Biomaterials* **2017**, *122*, 130−140.
(14) Chen, X.; Tian, X.; Shin, I.; Yoon, J. *Chem. Soc. Rev.* **2011**, *40*, 4783−4804.
(15) Ye, S.; Hu, J. J.; Yang, D. *Angew. Chem., Int. Ed.* **2018**, *57*, 10173−10177.
(16) Dickinson, B. C.; Lin, V. S.; Chang, C. J. *Nat. Protoc.* **2013**, *8*, 1249−1259.
(17) Zhang, W.; Liu, W.; Li, P.; Huang, F.; Wang, H.; Tang, B. *Anal. Chem.* **2015**, *87*, 9825−9828.
(18) Abo, M.; Urano, Y.; Hanaoka, K.; Terai, T.; Komatsu, T.; Nagano, T. *J. Am. Chem. Soc.* **2011**, *133*, 10629.
(19) Yik-Sham Chung, C.; Timblin, G. A.; Saijo, K.; Chang, C. J. *J. Am. Chem. Soc.* **2018**, *140*, 6109−6121.
(20) Zhou, Y.; Pei, W.; Zhang, X.; Chen, W.; Wu, J.; Yao, C.; Huang, L.; Zhang, H.; Huang, W.; Chye Loo, J. S.; Zhang, Q. *Biomaterials* **2015**, *54*, 34−43.
(21) Lippert, A. R.; Van de Bittner, G. C.; Chang, C. J. *Acc. Chem. Res.* **2011**, *44*, 793−804.
(22) Sun, X.; Xu, Q.; Kim, G.; Flower, S. E.; Lowe, J. P.; Yoon, J.; Fossey, J. S.; Qian, X.; Bull, S. D.; James, T. D. *Chem. Sci.* **2014**, *5*, 3368−3373.
(23) Kim, D.; Kim, G.; Nam, S. J.; Yin, J.; Yoon, J. *Sci. Rep.* **2015**, *5*, 8488−8496.
(24) Sun, W.; Guo, S.; Hu, C.; Fan, J.; Peng, X. *Chem. Rev.* **2016**, *116*, 7768−7817.
(25) Olney, J. W.; Tenkova, T.; Dikranian, K.; Muglia, L. J.; Jermakowicz, W. J.; D'Sa, C.; Roth, K. A. *Neurobiol. Dis.* **2002**, *9*, 205−219.
(26) O'Keefe, J.; Nadel, L. *Science* **1979**, *204*, 762.
(27) Agrawal, H. C.; Davis, J. M.; Himwich, W. A. *J. Neurochem.* **1968**, *15*, 917−923.
(28) Guo, Z.; Park, S.; Yoon, J.; Shin, I. *Chem. Soc. Rev.* **2014**, *43*, 16−29.
(29) Yuan, L.; Lin, W.; Zheng, K.; He, L.; Huang, W. *Chem. Soc. Rev.* **2013**, *42*, 622−661.
(30) Han, X.; Song, X.; Yu, F.; Chen, L. *Adv. Funct. Mater.* **2017**, *27*, 1700769.
(31) Dou, K.; Chen, G.; Yu, F.; Liu, Y.; Chen, L.; Cao, Z.; Chen, T.; Li, Y.; You, J. *Chem. Sci.* **2017**, *8*, 7851−7861.
(32) Gao, M.; Wang, R.; Yu, F.; Chen, L. *Biomaterials* **2018**, *160*, 1−14.
(33) Chen, G.; Fu, Q.; Yu, F.; Ren, R.; Liu, Y.; Cao, Z.; Li, G.; Zhao, X.; Chen, L.; Wang, H.; You, J. *Anal. Chem.* **2017**, *89*, 8509−8516.
(34) Maeda, H.; Fukuyasu, Y.; Yoshida, S.; Fukuda, M.; Saeki, K.; Matsuno, H.; Yamauchi, Y.; Yoshida, K.; Hirata, K.; Miyamoto, K. *Angew. Chem., Int. Ed.* **2004**, *43*, 2389−2391.
(35) Tang, B.; Yu, F.; Li, P.; Tong, L.; Duan, X.; Xie, T.; Wang, X. *J. Am. Chem. Soc.* **2009**, *131*, 3016.
(36) Bos, M.; Mendelsohn, J.; Kim, Y. M.; Albanell, J.; Fry, D. W.; Baselga, J. *Clin. Cancer Res.* **1997**, *3*, 2099−2106.
(37) Gill, G. N.; Lazar, C. S. *Nature* **1981**, *293*, 305−307.
(38) Bae, Y. S.; Kang, S. W.; Seo, M. S.; Baines, I. C.; Tekle, E.; Chock, P. B.; Rhee, S. G. *J. Biol. Chem.* **1997**, *272*, 217−221.
(39) Veal, E. A.; Day, A. M.; Morgan, B. A. *Mol. Cell* **2007**, *26*, 1−14.
(40) Powis, G.; Bonjouklian, R.; Berggren, M. M.; Gallegos, A.; Abraham, R.; Ashendel, C.; Zalkow, L.; Matter, W. F.; Dodge, J.; Grindey, G. *Cancer Res.* **1994**, *54*, 2419−2423.
(41) Stefanska, J.; Pawliczak, R. *Mediators Inflammation* **2008**, *2008*, 106507.
(42) Turner, C. H.; Takano, Y.; Owan, I.; Murrell, G. A. *Am. J. Physiol.* **1996**, *270*, E634−E639.
(43) Franke, T. F.; Yang, S. I.; Chan, T. O.; Datta, K.; Kazlauskas, A.; Morrison, D. K.; Kaplan, D. R.; Tsichlis, P. N. *Cell* **1995**, *81*, 727−736.
(44) Miller, E. W.; Tulyathan, O.; Isacoff, E. Y.; Chang, C. J. *Nat. Chem. Biol.* **2007**, *3*, 263−267.
(45) Dierkes, R.; Warnking, K.; Liedmann, S.; Seyer, R.; Ludwig, S.; Ehrhardt, C. *PLoS One* **2014**, *9*, No. e88520.
(46) Dickinson, B. C.; Peltier, J.; Stone, D.; Schaffer, D. V.; Chang, C. J. *Nat. Chem. Biol.* **2011**, *7*, 106−112.

DOI: 10.1021/acs.analchem.8b05326
Anal. Chem. 2019, 91, 1203−1210